OPEN ACCESS
IOP Publishing

Made open access 12 March 2020
Journal of Physics: Condensed Matter

J. Phys.: Condens. Matter **31** (2019) 485301 (8pp)
https://doi.org/10.1088/1361-648X/ab3aa5

Commensurability and quantum interference magnetotransport oscillations in a two-dimensional electron gas sandwiched by superconductors

Y Takagaki

Paul-Drude-Institut für Festkörperelektronik, Leibniz-Institut im Forschungsverbund Berlin e. V., Hausvogteiplatz 5-7, 10117 Berlin, Germany

E-mail: takagaki@pdi-berlin.de

Received 29 April 2019, revised 19 June 2019
Accepted for publication 13 August 2019
Published 30 August 2019

Abstract

Magnetic-field dependence of the transport properties of ballistic two-dimensional electrons in a planar superconductor–normal-conductor–superconductor structure is numerically investigated. In the circumstance where the Andreev reflection from the normal-conductor–superconductor interfaces is almost perfect, two oscillatory behaviors occur for magnetic fields higher and lower than that for the coincidence of the cyclotron diameter with the separation between the superconductors. The oscillation period for the former and latter cases is proportional to the magnetic field and inverse of the magnetic field, respectively. The low-field oscillation originates from commensurability-driven guiding of Andreev-reflected trajectories along the interfaces between the normal conductor and the superconductors. If the Andreev reflection probability is considerably less than unity, the commensurability oscillation is suppressed in amplitude and is dwarfed by additionally emerged oscillations originating from the quantum interference between the Andreev- and normal-reflected components.

Keywords: normal-conductor–superconductor hybrid structure, Andreev reflection, magnetotransport oscillations, commensurability, quantum interference effects

(Some figures may appear in colour only in the online journal)

1. Introduction

The transport properties in junctions of normal conductors and superconductors are described in terms of quasiparticle excitations around the Fermi level in the normal-conductor segment [1, 2]. The current in the bulk of the superconductor is carried by Cooper pairs. In order to satisfy the continuity across the normal-conductor–superconductor (NS) interface, an electronlike excitation incident from the normal conductor with an energy ε above the Fermi energy μ is reflected from the interface as a holelike excitation with the energy below μ by ε, as known as Andreev reflection. Here, the quasiparticle excitation is completely reflected from the NS interface under the condition that 2ε is smaller than the superconducting gap Δ.

When a magnetic field B is applied to the normal conductor, the electronlike excitation undergoes cyclotron orbital motion. The holelike excitation that is Andreev-reflected from the NS interface acts as if a positively-charged particle were subjected to a magnetic field $-B$. Consequently, instead of the holelike excitation tracing back the trajectory of the incident electronlike excitation, the quasiparticle excitations propagate along the NS interface in the manner of a skipping orbit, where the type of the quasiparticle excitation changes alternately between being electronlike and holelike after each Andreev reflection [3]. As the length L of the NS interface

is finite in real devices, the quasiparticle excitation incident, for instance, as being electronlike leaves the NS interface as a holelike or electronlike excitation depending on whether the number of Andreev reflections, which is given by $L/(2r_c)$ with r_c being the cyclotron radius, is odd or even integers, respectively. A periodic magnetic-field dependence emerges for the differential conductance G_{NS} of the NS junction [3] as it is related to the Andreev reflection as [4, 5]

$$G_{NS} = \frac{4e^2}{h}\mathrm{Tr}[s_{he}s_{he}^{\dagger}], \tag{1}$$

where s_{he} is the scattering matrix for an electronlike excitation leaving the system as a holelike excitation.

Recently, Delfanazari *et al* [6] reported a conductance modification by magnetic field in an NS hybrid device that was in the form of a planar Josephson junction. A high-mobility two-dimensional electron gas (2DEG) created in an (In,Ga)As quantum well was attached there to Nb superconducting contacts. Interestingly, the modulation appeared at low magnetic fields where the cyclotron radius of the 2DEG $r_c = \hbar k_F/(eB)$ was larger than the separation W between the superconductors. Here, $k_F = (2\pi n_s)^{1/2}$ is the Fermi wavenumber with n_s being the sheet concentration of the 2DEG. As quasiparticle excitations are reflected from both of the NS interfaces, the oscillation mechanism in [3] for a single NS interface is not applicable.

In this paper, the magnetotransport properties in a superconductor–normal-conductor–superconductor (SNS) structure are theoretically investigated. Attentions are focused on the circumstance where the quasiparticle excitations are Andreev-reflected from the two parallel NS interfaces. In addition to the conventional magnetotransport oscillation [3] that appears at high magnetic fields for $r_c < W$, another oscillation that is periodic in $1/B$ is found for $r_c > W$. A guided drift motion of the Andreev-reflected quasiparticle excitations is shown to occur in the billiard of ballistic electrons within the superconductor confinement. Its origin is revealed to be the commensurability in a periodic configuration of unfolded NS interfaces. It is shown additionally that the observation of the commensurability oscillation requires nearly perfect Andreev reflection from the NS interfaces. The low-magnetic-field behavior is dominated by quantum interference effects by producing additional oscillations when normal reflection coexists.

2. Model

Figure 1 illustrates the device geometry investigated in the present work. The uniform strip of a 2DEG having a width of W is sandwiched by two superconductors, which are shown as gray areas. The distance between the superconductors is, therefore, W. The 2DEG is contacted by the superconductors over a length of L. Transport coefficients are considered below for the quasiparticle excitations in the normal segment. When an electronlike excitation is incident from the left-hand side of the 2DEG strip into the scattering region composed of the NS-interfaces, it is either transmitted or reflected. For each

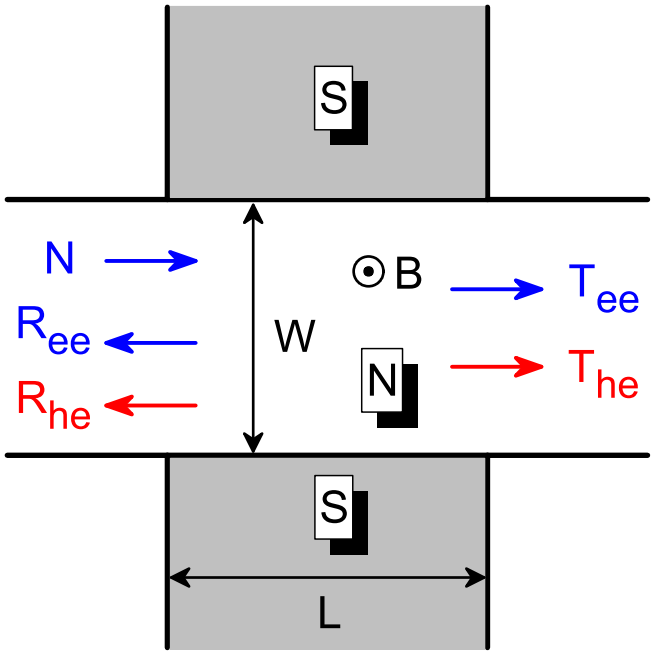

Figure 1. Superconductor–normal-conductor–superconductor structure. The horizontal channel with a width of W is made of a two-dimensional electron gas. The normal conductor 'N' is contacted by two superconductors 'S', which are shown as gray semi-infinite strips. The length of the interface between the normal conductor and the superconductors is L. The transport coefficients R_{ee}, R_{he}, T_{ee} and T_{he} are calculated when an electronlike excitation is injected to the scattering region. The blue and red colors correspond to the electronlike and holelike excitations, respectively. The number of the incident modes is N in the quantum-mechanical situation. The excitation energy ε is assumed to be zero, and so the quasiparticle excitations are completely reflected from the superconductors. A magnetic field B is applied perpendicular to the plane.

case, the quasiparticle excitation can leave the region as being electronlike or holelike. There are, therefore, four scattering coefficients T_{ee}, T_{he}, R_{ee} and R_{he}, as shown in figure 1. Here, R_{he}, for instance, is the probability that the incident electronlike excitation is reflected as a holelike excitation.

In the experiment by Delfanazari *et al* [6], the differential conductance of the SNS structure was measured using the superconductors as the source and drain of the current. Because of the proximity between the two superconductors, the system ought to be treated ideally as a Josephson junction [7–9]. It is assumed here that the superconducting coupling is negligible, and so the system is regarded as a series of two NS junctions. To be specific, the critical current associated with the Josephson coupling is assumed to be below the current used to measure the conductance of the SNS structure due to, for instance, a large distance between the superconductors. The conductance G_{SNS} of the system is thus approximately given as $G_{SNS} \approx (1/2)G_{NS}$. The conductance G_{NS} of one NS junction is determined by the Andreev reflection as $G_{NS} = (4e^2/h)r_{he}$. The Andreev reflection probability r_{he} for one NS interface is anticipated to behave roughly as $r_{he} \sim R_{he} + T_{he}$. That is, the incident electronlike excitation leaves the system as a holelike excitation either in the backward or forward propagation.

The quantum transmission of the quasiparticle excitations is examined in the presence of a perpendicular magnetic field by solving the Bogoliubov–de Gennes equation [1]

$$\begin{bmatrix} H_0 & \Delta(x,y) \\ \Delta^*(x,y) & -H_0^* \end{bmatrix} \begin{pmatrix} u \\ v \end{pmatrix} = \varepsilon \begin{pmatrix} u \\ v \end{pmatrix}, \qquad (2)$$

where $u(x,y)$ and $v(x,y)$ are the wavefunctions of, respectively, the electronlike and holelike excitations and $H_0 = (p - eA)^2/(2m) + U - \mu$ is the single-particle Hamiltonian with $U(x,y)$ and $A(x,y)$ being the electrostatic and vector potentials, respectively. The transport coefficients were calculated using the modal expansion method [3, 10]. The number of the incident modes is N in the quantum-mechanical situation, and so $T_{ee} + T_{he} + R_{ee} + R_{he} = N$. For simplicity, the magnetic field in the superconductor regions is assumed to be zero, see appendix.

3. Commensurability oscillation

This section is devoted to a situation where the Andreev reflection at the NS interface is almost perfect and thus the normal reflection is negligible. To realize such a situation [3], μ is assumed to be identical in the 2DEG and the superconductors and Δ is chosen to be much smaller than μ, i.e. $\Delta/\mu = 0.01$. In addition, the bias voltage V applied between the superconductors to measure the conductance is assumed to be small, and so $\varepsilon = eV/2$ is set to be 0 throughout the paper.

The magnetic-field dependence of the transport coefficients is plotted in figure 2(a) for $k_F W/\pi = 13.6$ and $L/W = 3.6$. The abscissa W/r_c is proportional to B. The oscillation in high magnetic fields is due to the mechanism in [3]. For the condition $r_c < W$, the quasi-particle excitations are reflected from only one NS interface, as illustrated in the inset. The incident quasiparticle excitation is forward transmitted along the NS interface without backscattering in the manner of the edge state. The electronlike and holelike excitations switch with each other after each Andreev reflection, resulting in an out-of-phase oscillation in T_{ee} and T_{he}. The top scale shows that the oscillation period is $\delta(L/r_c) = 4$, as expected for this oscillation.

An oscillation of another type emerges at low magnetic fields $W/r_c < 1$. As evident in figure 2(c), this oscillation is periodic in $1/B$ with the period $\delta(r_c/W) = 1$. From the condition $r_c > W$ for the appearance of the oscillation, it is obvious that simultaneous Andreev reflections from both of the NS interfaces play an important role. An example of the Andreev-reflected trajectory in this circumstance is shown in figure 3(a). Here, the trajectory starts from 'S' and ends at 'E'. The blue and red curves correspond to the electronlike and holelike excitations, respectively. In this case of $r_c/W = 3.4$, the trajectory propagates backward in comparison to the conventional propagation direction of the edge state. The anomalous propagation by the guiding along the NS interfaces is the origin of the magnetotransport oscillation [11]. The importance of the guided drift motion for the phenomenon is affirmed by the simulations in figure 4, where the ratio L/W was varied. As the NS interface becomes longer, the guiding

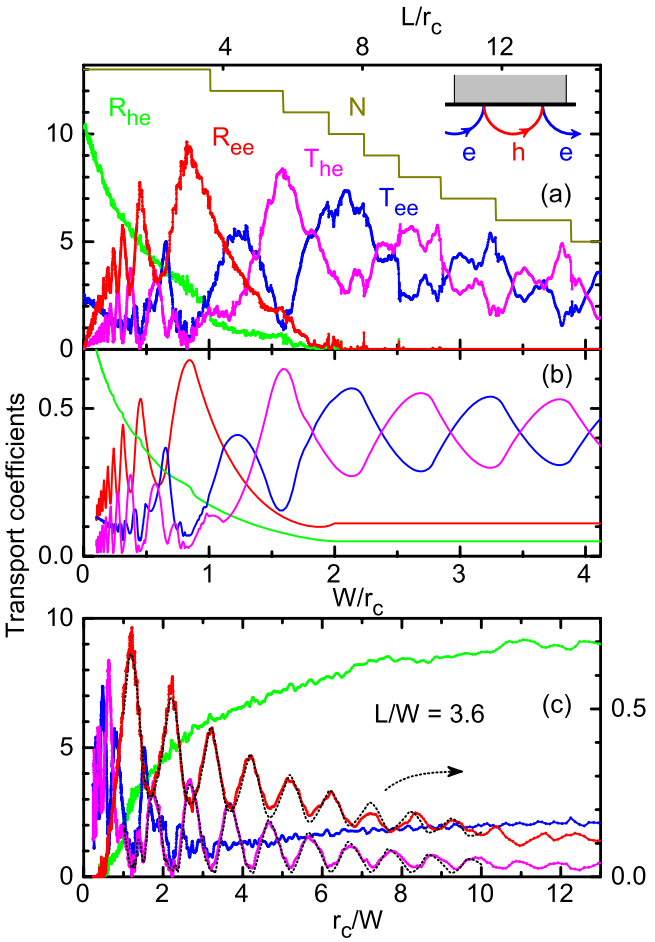

Figure 2. Magnetic-field dependence of transport coefficients R_{ee}, R_{he}, T_{ee} and T_{he} in SNS structure. The abscissa W/r_c for (a) and (b) is proportional to the magnetic field, where W is the width of the normal-conductor strip and r_c is the cyclotron radius. The ratio L/W is 3.6. For the quantum-mechanical calculations in (a), $k_F W/\pi = 13.6$, $\Delta/\mu = 0.01$ and $\varepsilon = 0$ were assumed. The curves in (b) were calculated using the classical billiard model assuming perfect Andreev reflection from the superconductors. The out-of-phase high-magnetic-field oscillations in T_{ee} and T_{he} originate from the skipping orbit illustrated in the inset of (a), where the blue and red curves correspond to the electronlike and holelike excitations, respectively. The gray area represents the superconductor segment. These results are shown in terms of r_c/W in (c), i.e. the dependence on the inverse of the magnetic field. The quantum-mechanical results are shown by the colored solid curves. The dotted curves show the corresponding classical results for R_{ee} and T_{he}.

of the trajectory is better established. The oscillation is consequently enhanced in amplitude.

Let me now examine the guiding of the trajectory in detail. The incidence angle of the quasiparticles with respect to the NS interface is preserved in the Andreev reflection. The guided trajectory in the strip with the width W is hence equivalent to a semicircle cyclotron orbit with radius r_c, which is shown in figure 3(b) as the green curve, through a procedure of unfolding the trajectory by mirror-reflections at the NS interfaces. It is crucial to recognize that the trajectory needs to be flipped additionally in the horizontal direction for the branches of the electronlike excitation in constructing the guided trajectory from the semicircle orbit. This flip in the horizontal direction enables the backward propagation. The number of reflections from the NS

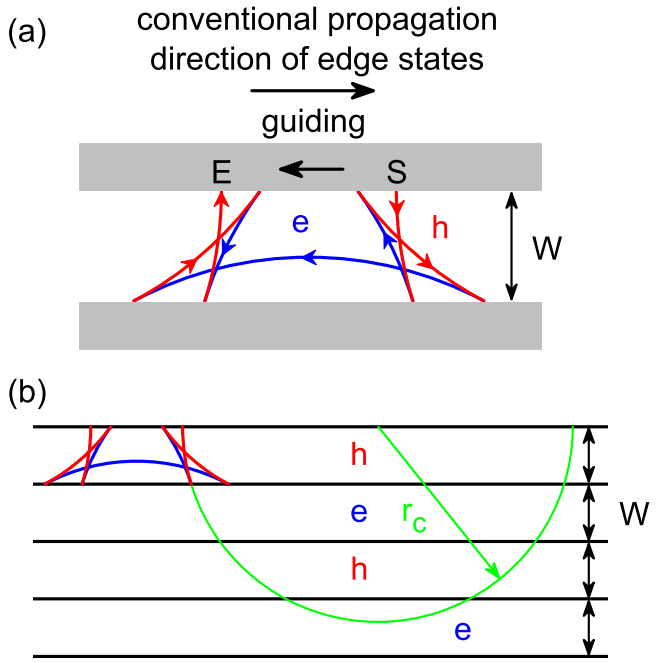

Figure 3. Classical Andreev-reflected trajectory in a SNS structure. Quasiparticle excitations are confined in the normal conductor sandwiched by superconductors as shown in (a). The width of the normal-conductor strip is W. The superconductors are shown as gray areas. The incident electronlike excitation is Andreev-reflected to a holelike excitation at the starting point 'S'. The cycle ends at point 'E'. The blue and red curves correspond to the electronlike and holelike excitations, respectively. The application of a magnetic field causes a guiding motion, whose propagation direction is opposite to that of the conventional edge state in this example. The Andreev-reflected trajectory is constructed by folding the semicircle orbit and having a radius of r_c, which is shown by the green curve in (b), with respect to the normal-conductor–superconductor interfaces expressed as black horizontal lines. Here, the trajectory needs to be flipped horizontally in addition to the folding in the vertical direction for the segments of the electronlike excitation.

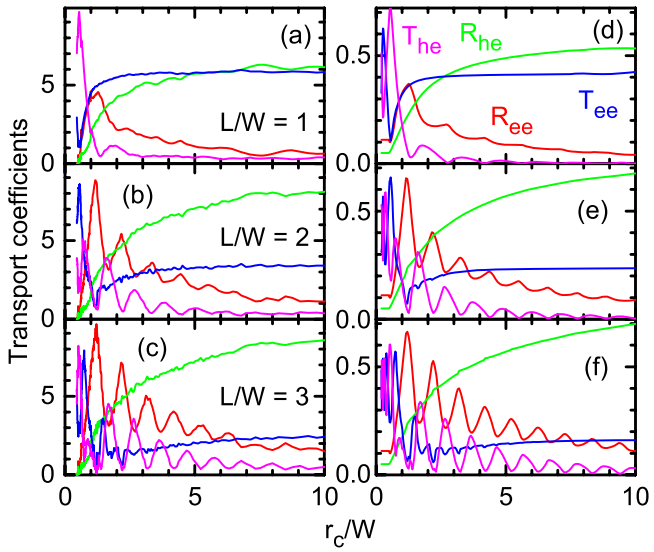

Figure 4. Magnetotransport coefficients R_{ee}, R_{he}, T_{ee} and T_{he} in a SNS structure as a function of L/W. The geometry ratio L/W is 1 for (a) and (d), 2 for (b) and (e) and 3 for (c) and (f). The coefficients were calculated quantum-mechanically in (a)–(c) and classically in (d)–(f). The parameters for the quantum-mechanical calculations were $k_F W/\pi = 13.6$, $\Delta/\mu = 0.01$ and $\varepsilon = 0$.

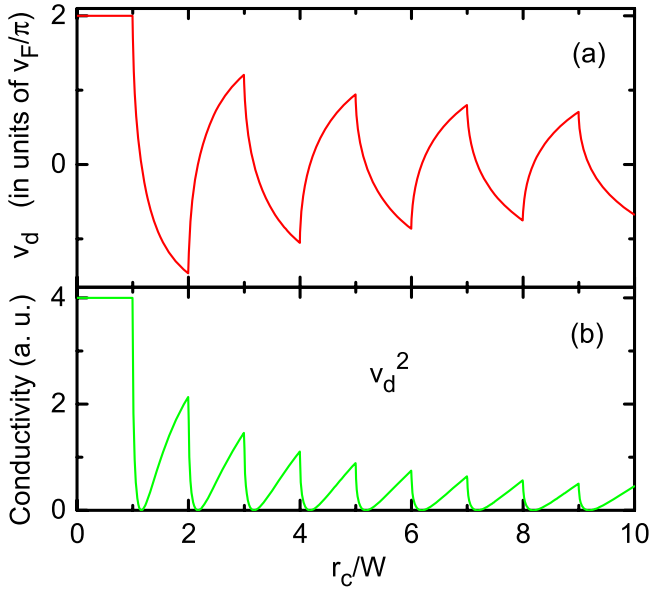

Figure 5. Dependencies of (a) guiding drift velocity v_d and (b) conductivity on inverse of magnetic field in a SNS structure. The velocity v_d calculated using the classical model for the representative trajectory shown in figure 3 is normalized by the Fermi velocity v_F. The conductivity of the system is assumed to be proportional to v_d^2 in (b).

interfaces in the one cycle such as that displayed in figure 3(a) is $2r_c/W$. Among the branches of the semicircle orbit sliced by the width W, those in the upper segments stretch mainly in the vertical direction. Their contribution for the guiding motion is, therefore, insignificant and roughly cancels out. The direction of the guided drift motion of the Andreev-reflected trajectory is mainly determined by the bottom segment. The quasiparticle in the bottom segment changes between being electronlike and holelike when r_c/W is varied. As a consequence, the drifting direction along the NS interface changes periodically. The guiding in the forward (backward) direction becomes maximal when r_c/W is odd (even) integers.

In figure 5(a), the dependence on r_c/W of the guiding drift velocity v_d normalized by the Fermi velocity v_F is plotted. The velocity was calculated for the representative classical trajectory illustrated in figure 3, for which the quasiparticle excitation was initially injected perpendicular to the NS interface. The drifting direction changes alternately with a period of $\delta(r_c/W) = 2$. The period of the oscillation in the transport coefficients is, however, $\delta(r_c/W) = 1$. The magnetotransport modulation is thus indicated to occur based on whether the quasiparticle excitations are localized or mobile, independent of the propagation direction. To summarize, the guided drift motion driven by a commensurability in the periodic system depicted in figure 3(b) is responsible for the oscillation. The phenomenon is thus similar to the Weiss oscillation that appears when a one-dimensional periodic potential is imposed on the 2DEG [12–14]. Following the formulation for the Weiss oscillation by Beenakker [15], the conductivity σ of the SNS system in the limit of $L \to \infty$ is related by the Einstein relation to the diffusion coefficient D as $\sigma \propto D$. As D depends on v_d in the manner of $D \propto v_d^2$, σ is given as shown in figure 5(b).

Given that the guiding of the classical trajectory is responsible for the magnetotransport modulation, the behavior is expected to be produced even by a classical simulation instead of the quantum-mechanical one. The transport coefficients were, therefore, calculated also using the classical billiard model [16]. The results are plotted in figures 2(b), (c) and 4(d)–(f). The excellent agreement with the corresponding quantum-mechanical results confirms the classical origin of the oscillation.

For simplicity, $\varepsilon = 0$ was assumed in the simulations. The quasiparticle excitations remain to be completely reflected from the superconductors so long as $\varepsilon < \Delta/2$. The magnetotransport oscillations survive even if ε is finite as $0 < \varepsilon < \Delta/2$, see [3]. Modifications occur nonetheless as the cyclotron radius is no longer the same between the electronlike and holelike excitations. They are, however, small due to the circumstance $\Delta \ll \mu$ assumed in the present paper.

The low-magnetic-field oscillation appears dominantly in $R_{\rm ee}$ and $T_{\rm he}$ in the circumstance of the present simulations and no modulation is exhibited in $R_{\rm he}$. Nevertheless, the conductance of the system is roughly anticipated to be given by $r_{\rm he} \sim R_{\rm he} + T_{\rm he}$. It is thus reasonable to attribute the magnetotransport modulation reported by Delfanazari *et al* [6] to the oscillation revealed in the present work. It may be noteworthy in this respect that the modulation was superimposed in [6] on a background conductance that rapidly decayed as the magnetic field increased. In the aforementioned interpretation, the behavior of the background is ascribed to the monotonic decrease of $R_{\rm he}$, which occurs as the reflection vanishes when the magnetic field is increased to realize the condition $2r_{\rm c} < W$.

In figures 2 and 4, one notices for the quantum-mechanical results that irregular fluctuations are superimposed on the behavior having the classical origin. These fluctuations are attributed to the quantum interference associated with multiple reflections within the SNS segment caused by the quantum-mechanical scattering at the abrupt appearance and disappearance of the superconductors. The commensurability oscillation vanishes in experimental situations if the mean free path is not sufficiently long. The fluctuations will, on the other hand, remain provided that the phase coherence is maintained at a low temperature. The possibility of the magnetoconductance modification in [6] resulting from the fluctuations rather than the commensurability oscillation is ruled out, however, as the fluctuations are not restricted to the low-magnetic-field regime. Although the adiabatic transport of edge states is already established at high magnetic fields in the sense that the backscattering vanishes, i.e. $R_{\rm ee} \approx R_{\rm he} \approx 0$, the scattering can still take place as a transition between the electronlike and holelike states.

In comparing the numerical results with the experimental observation by Delfanazari *et al* [6], it is necessary to pay attention to the difference between the model geometry in figure 1 and the experimental device. The length of the NS interface is exactly the length of the SNS segment in the simulations. The separation between the two NS interfaces was, in contrast, widened gradually in the experimental device outside of the SNS segment having the constant width W. A consequence of this difference is that the $\delta(L/r_{\rm c}) = 4$ oscillation at high magnetic fields cannot be expected for the experimental device as the oscillation period is determined not by L but by the total length of the NS interface, which was presumably longer than the mean free path of the 2DEG. This geometry difference is, however, not important for the low-magnetic-field oscillation. A modification occurs, nonetheless, that the incident quasiparticle excitation can enter the narrow segment both as being electronlike and holelike depending on the number of the Andreev reflections that the quasiparticle excitation experiences prior to entering the narrow segment. The oscillation appears in this situation in all of the four transport coefficients.

Concerning the issue why the oscillation appears only in $R_{\rm ee}$ and $T_{\rm he}$, it may be explained as follows. In the Andreev trajectories for the device geometry displayed in figure 1, the quasiparticle excitation enters the SNS section as an electronlike excitation. The electronlike excitation becomes a holelike excitation after the first Andreev reflection and moves further in the forward direction. It is noticed that the propagation direction for the branches of the holelike excitation is always forward, whereas it is always backward for those of the electronlike excitation. If the quasiparticle excitation finally leaves the SNS segment as being reflected, it will likely leave the system as an electronlike excitation. When the quasiparticle excitation leaves the SNS segment as being transmitted, on the other hand, it will likely leave the system as a holelike excitation.

4. Effects of imperfection of Andreev reflection

In this section, consequences on the magnetotransport properties are examined when the Andreev reflection from the NS interface is not perfect and so the normal reflection coexists. Partial normal reflection was introduced in the theory in [1] by incorporating a δ-function-type repulsive potential at the NS interface. It should be emphasized that the coexistence of the normal reflection cannot be avoided in reality even if the NS interface is perfect and no potential barrier exists because of the fact that the Fermi energy in the superconductor is much larger than that in the 2DEG and also the carrier effective mass is different between the superconductor and the 2DEG. The simulations are, therefore, carried out here with a condition that the Fermi energy μ_S in the superconductors is larger than the Fermi energy μ_N in the 2DEG.

Figure 6 compares the transport characteristics when the ratio μ_S/μ_N was varied to be 1 in (a), 1.7 in (b) and 4 in (c) for $L/W = 3$. As μ_S becomes larger than μ_N, the normal component in the reflection from the NS interface increases. The commensurability oscillation is consequently reduced in amplitude. More importantly, an oscillation emerges at the intermediate magnetic field range between the commensurability oscillation for $W/r_{\rm c} < 1$ and the high-field oscillation due to the Andreev skipping orbit, i.e. at $W/r_{\rm c} \sim 1.5$ in figure 6(c). Instead of the commensurability oscillation, the new oscillation dominates the transport characteristics for $\mu_S/\mu_N = 4$. This oscillation originates from the quantum interference between the Andreev- and normal-reflected components, as illustrated in the inset of figure 6(c) [3, 17–19]. The

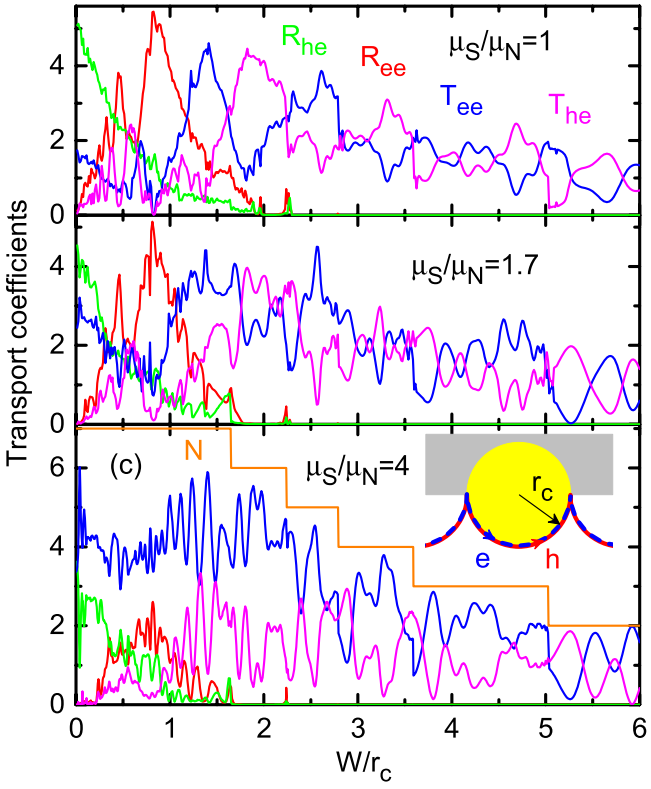

Figure 6. Magnetotransport coefficients R_{ee}, R_{he}, T_{ee} and T_{he} in a SNS structure when perfection of Andreev reflection is deteriorated by increasing μ_S/μ_N. The normal reflection at the NS interfaces increases as the Fermi energy μ_S in the superconductors is larger than the Fermi energy μ_N in the 2DEG. The calculations were carried out with $k_F W/\pi = 8$, $L/W = 3$, $\Delta/\mu_S = 0.01$ and $\varepsilon = 0$.

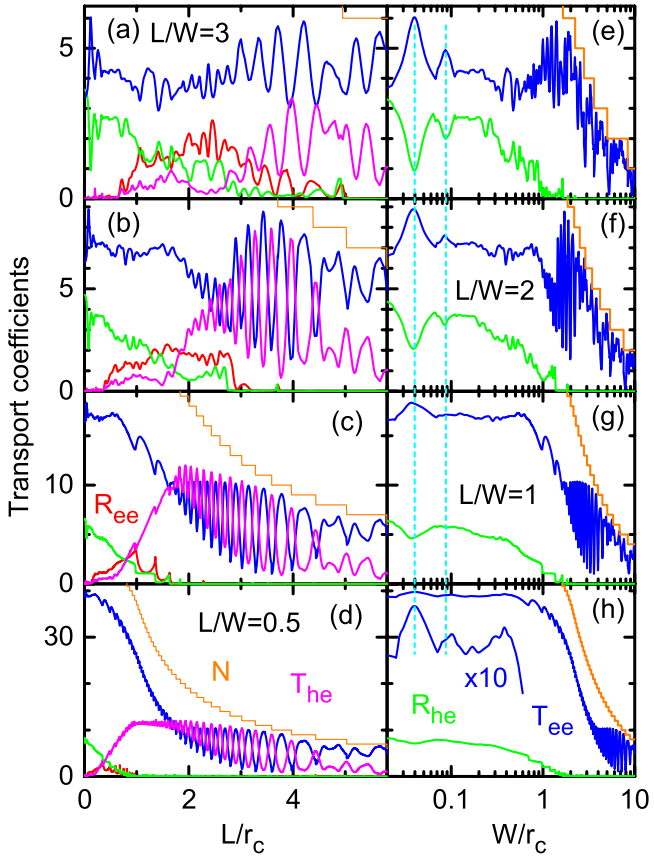

Figure 7. Variation of quantum interference effects with L/W when $\mu_S/\mu_N = 4$ and $k_F L/\pi = 24$. The geometry ratio L/W is 3 in (a) and (e), 2 in (b) and (f), 1 in (c) and (g) and 0.5 in (d) and (h). The magnetic-field dependence is plotted in terms of L/r_c in (a)–(d) and W/r_c in (e)–(h). The dashed lines in (e)–(h) indicate an oscillation at very low magnetic fields.

quantum interference oscillation is demonstrated in figure 7 for a number of values of the geometry ratio L/W for a fixed value of $k_F L/\pi = 24$.

An Aharonov–Bohm-type (AB-type) quantum interference between the Andreev- and normal-reflected components is responsible for the oscillation, where the phase shift is given by the magnetic flux enclosed by the cyclotron orbit, i.e. the yellow disk in the inset of figure 6(c)[1]. The primary oscillation period corresponds to adding a magnetic flux quantum $\phi_0 = h/e$ to the yellow area. This condition for the oscillation period is identical with the Landau level filling factor ν [19]. Specifically, $\nu/2 = \pi r_c^2 B/\phi_0$, where the factor 2 is the spin degeneracy. As a consequence, the oscillation minima (maxima) in T_{ee} (T_{he}) coincide with the magnetic depopulation of the Landau levels, as one finds in figures 7(c) and (d) when the quantum interference oscillation is most clearly developed at $L/r_c = 2$–4.

Alterations of the oscillation period occur at high magnetic fields. In figure 7, additional minima are generated in T_{ee} for $L/r_c > 4$ at the middles between the magnetic depopulation thresholds of the Landau levels. The oscillation period is consequently halved. The multiplication of the oscillation arises as the phase shift associated with a single cyclotron orbit is multiplied when the number of the orbits that fit in the length of L increases. It is remarkable that the first transition occurs rather abruptly at $L/r_c \sim 4$ in the form of the oscillation doubling. The multiplication of the oscillation takes place further with increasing L/r_c, similarly in the form of the doubling. In practice, the AB-type quantum interference is found to become insignificant at high magnetic fields, see figure 6. The doubling effect is consequently unimportant when $r_c \ll L$.

Deviations in the oscillation period occur also at low magnetic fields. The cyclotron orbit is scattered from both of the NS interfaces for $r_c > W$. The area that encloses the magnetic flux to determine the phase shift depends on r_c/W in a complicated manner. The oscillation thus exhibits irregular behavior, as evident in figure 7(a). In addition, the quasi-one-dimensional (quasi-1D) quantum confinement is stronger than the Landau quantization in this regime. The quantum interference oscillation in figure 7(b), as a consequence, does not coincide with the magnetic depopulations of the Landau levels. Furthermore, even when the AB-type quantum interference becomes negligible as the magnetic field further approaches zero, the magnetic depopulation of the quasi-1D subbands causes an oscillation-like behavior in the transport coefficients, see figures 7(c) and (d). These behaviors have implications in the experimental attempt to observe the commensurability oscillation. Careful analysis

[1] The statement regarding the phase shift associated with figure 5 in [3] is incorrect. See [17, 18].

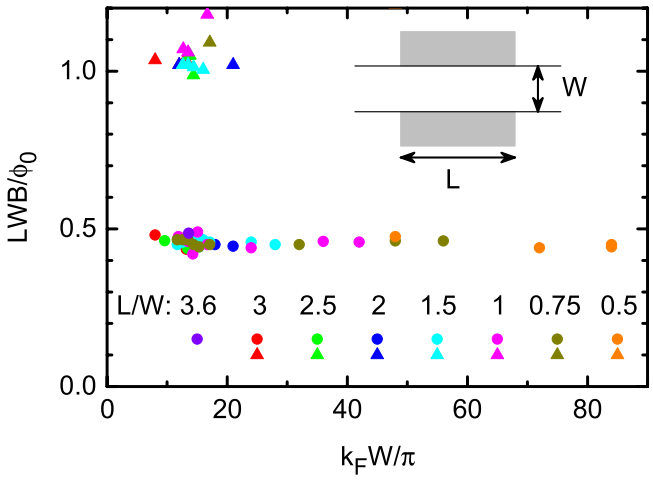

Figure 8. Magnetic-field values B at peaks in T_{ee} of oscillation at very low magnetic fields. The circles and triangles correspond, respectively, to the first and second peaks indicated by the dashed lines in figure 7. The values of L/W were as summarized at the bottom of the panel. The inset shows the length L and width W of the 2DEG sandwiched by the superconductors, which are illustrated as gray areas. The magnetic flux LWB in the sandwiched 2DEG area is divided by the magnetic flux quantum $\phi_0 = h/e$.

of the magnetic-field dependence is required to unambiguously identify the commensurability oscillation. Temperature dependence of the oscillation amplitude will provide useful information as, contrary to the classical commensurability oscillation, the quantum interference is suppressed with increasing the temperature due to dephasing.

I point out the existence of another oscillation at very low magnetic fields that is also associated with the imperfection of the Andreev reflection. This oscillation is marked by the dashed lines in figures 7(e)–(h). The oscillation amplitude decays with increasing the magnetic field, resembling the Altshuler–Aronov–Spivak (AAS) oscillation [20]. In figure 8, the position in B of the first and second peaks in T_{ee} is plotted in terms of LWB/ϕ_0, respectively, by circles and triangles when the parameters $k_F W/\pi$ and L/W were varied. It is indicated that the first and second peaks occur when the number of the magnetic flux quanta enclosed in the 2DEG area sandwiched by the superconductors is about one half and one, respectively. That the oscillation period is determined by $\phi_0/2$ is also similar to the AAS oscillation. In a real system, disorder inevitably exits. The disorder is expected to suppress the commensurability and AB-type oscillations as they are associated with scatteringless cyclotron orbits. It will be interesting to examine the effect of disorder on the AAS-like oscillation as the AAS oscillation, in fact, originates from the disorder and is insensitive to it [20].

At the interface between a graphene and a superconductor, not only the Andreev retroreflection considered above but also specular Andreev reflection takes place [21–23]. In the specular Andreev reflection, the Andreev-reflected holelike excitation propagates in the direction of the specular boundary reflection of the incident electronlike excitation. The unusual reflection occurs when an electronlike excitation in the conduction band is scattered into a holelike excitation in the valence band under the circumstance of the Fermi level in the graphene being located around the Dirac point. It will be interesting to investigate how the guiding drift motion in the commensurability oscillation is affected by the specular Andreev reflection.

5. Conclusions

In conclusion, the ballistic magnetotransport properties of quasiparticle excitations have been calculated using quantum-mechanical and classical methods for a planar superconductor–normal-conductor–superconductor structure. Provided that the Andreev reflection from the normal-conductor–superconductor (NS) interfaces is almost perfect, an oscillation that is periodic in the inverse of magnetic field emerges under the condition that the diameter of the cyclotron orbit is larger than the separation between the superconductors. A guided drift motion of classical trajectories that are Andreev-reflected from both of the NS interfaces has been identified to be responsible for the oscillation. When the Andreev reflection is considerably less than perfect, the quantum interferences between the Andreev- and normal-reflected components give rise to two additional oscillations. Together with the effect of the magnetic depopulation of quasi-1D subbands, these behaviors need to be carefully distinguished in the experimental confirmation of the oscillations.

Acknowledgments

I thank K Delfanazari for bringing the experimental observation to my attention.

Appendix. Gauge transformation

The magnetic field was assumed to be zero in the superconductors and present only in the normal conductor. Gauge transformations were used to obtain the wavefunctions in such a situation.

The normal-conductor strip in figure 1 was defined for $0 \leqslant y \leqslant W$. The two semi-infinite superconductor strips for $0 \leqslant x \leqslant L$ were attached to the normal-conductor strip as $y \leqslant 0$ and $y \geqslant W$. A vector potential $\mathbf{A} = (-By, 0, 0)$ was chosen for the magnetic field B. This allowed to describe the zero magnetic field in the lower superconductor strip with $y \leqslant 0$ as $\mathbf{A} = \mathbf{0}$. The pair potential in this strip was set to be $\Delta(x, y) = \Delta_0$. For the upper superconductor strip with $y \geqslant W$, $\Delta(x, y)$ was $\Delta_0 e^{i\varphi}$. (The superconducting phase difference φ was assumed to be zero in the numerical simulations.) The zero magnetic field in this strip was realized as $\mathbf{A} = (-BL, 0, 0) = (0, 0, 0) + \nabla(-BLx)$. For gauge transformation $\mathbf{A} \to \mathbf{A}' = \mathbf{A} + \nabla f$, the wavefunctions are given by

$$\begin{pmatrix} u(x,y) \\ v(x,y) \end{pmatrix} \to \begin{pmatrix} u'(x,y) \\ v'(x,y) \end{pmatrix} = \begin{pmatrix} e^{-i\frac{e}{\hbar}f} u(x,y) \\ e^{+i\frac{e}{\hbar}f} v(x,y) \end{pmatrix} \quad (A.1)$$

with

$$\Delta \to \Delta' = \mathrm{e}^{-2\mathrm{i}\frac{e}{\hbar}f}\Delta. \tag{A.2}$$

The quantized modes in the superconductor strip are

$$\begin{pmatrix} u_n(x,y) \\ v_n(x,y) \end{pmatrix} \propto \mathrm{e}^{\mathrm{i}k_n y}\sqrt{\frac{2}{L}}\sin\left(\frac{n\pi}{L}x\right)\begin{pmatrix}\gamma \\ 1\end{pmatrix}, \tag{A.3}$$

where

$$k_n = \left[\frac{2m}{\hbar^2}\mu - \left(\frac{n\pi}{L}\right)^2 + \mathrm{i}\frac{2m}{\hbar^2}\sqrt{\Delta_0^2 - \varepsilon^2}\right]^{1/2} \tag{A.4}$$

and

$$\gamma = \frac{\varepsilon + \mathrm{i}\sqrt{\Delta_0^2 - \varepsilon^2}}{\Delta_0}\mathrm{e}^{\mathrm{i}\varphi}. \tag{A.5}$$

ORCID iDs

Y Takagaki https://orcid.org/0000-0002-6691-1005

References

[1] Blonder G E, Tinkham M and Klapwijk T M 1982 Transition from metallic to tunneling regimes in superconducting microconstrictions: excess current, charge imbalance, and supercurrent conversion *Phys. Rev.* B **25** 4515–32

[2] Lambert C J, Hui V C and Robinson S J 1993 Multi-probe conductance formulae for mesoscopic superconductors *J. Phys.: Condens. Matter* **5** 4187–206

[3] Takagaki Y 1998 Transport properties of semiconductor–superconductor junctions in quantizing magnetic fields *Phys. Rev.* B **57** 4009–16

[4] Takane Y and Ebisawa H 1992 Conductance formula for mesoscopic systems with a superconducting segment *J. Phys. Soc. Japan* **61** 1685–90

[5] Lambert C J 1991 Generalized Landauer formulae for quasi-particle transport in disordered superconductors *J. Phys.: Condens. Matter* **3** 6579–87

[6] Delfanazari K *et al* 2018 Proximity induced superconductivity in indium gallium arsenide quantum wells *J. Magn. Magn. Mater.* **459** 282–4

[7] Zyuzin A Y 1994 Superconductor–normal-metal–superconductor junction in a strong magnetic field *Phys. Rev.* B **50** 323–9

[8] Ishikawa Y and Fukuyama H 1999 Effects of magnetic field on Josephson current in SNS system *J. Phys. Soc. Japan* **68** 954–63

[9] Baxevanis B, Ostroukh V P and Beenakker C W J 2015 Even-odd flux quanta effect in the Fraunhofer oscillations of an edge-channel Josephson junction *Phys. Rev.* B **91** 041409

[10] Takagaki Y and Tokura Y 1996 Transmission resonances in a semiconductor–superconductor junction quantum interference structure *Phys. Rev.* B **54** 6587–99

[11] Galaĭko V P and Bezuglyĭ E V 1971 Magnetic quantization and absorption of ultrasound in superconductors in the intermediate state *Sov. Phys.—JETP* **33** 796–801

[12] Weiss D, von Klitzing K, Ploog K and Weimann G 1989 Magnetoresistance oscillations in a two-dimensional electron gas induced by a submicrometer periodic potential *Europhys. Lett.* **8** 179–84

[13] Gerhardts R R, Weiss D and von Klitzing K 1989 Novel magnetoresistance oscillations in a periodically modulated two-dimensional electron gas *Phys. Rev. Lett.* **62** 1173–6

[14] Winkler R W, Kotthaus P and Ploog K 1989 Landau band conductivity in a two-dimensional electron system modulated by an artificial one-dimensional superlattice potential *Phys. Rev. Lett.* **62** 1177–80

[15] Beenakker C W J 1989 Guiding-center-drift resonance in a periodically modulated two-dimensional electron gas *Phys. Rev. Lett.* **62** 2020–3

[16] Beenakker C W J and van Houten H 1989 Billiard model of a ballistic multiprobe conductor *Phys. Rev. Lett.* **63** 1857–60

[17] Asano Y and Kato T 2000 Andreev reflection and cyclotron motion of a quasiparticle in high magnetic fields *J. Phys. Soc. Japan* **69** 1125–35

[18] Asano Y 2000 Magnetoconductance oscillations in ballistic semiconductor–superconductor junctions *Phys. Rev.* B **61** 1732–5

[19] Hoppe H, Zülicke U and Schön G 2000 Andreev reflection in strong magnetic fields *Phys. Rev. Lett.* **84** 1804–7

[20] Aronov A G and Sharvin Y V 1987 Magnetic flux effects in disordered conductors *Rev. Mod. Phys.* **59** 755–79

[21] Beenakker C W J 2006 Specular Andreev reflection in graphene *Phys. Rev. Lett.* **97** 067007

[22] Cheng S, Xing Y, Wang J and Sun Q 2009 Controllable Andreev retroreflection and specular Andreev reflection in a four-terminal graphene-superconductor hybrid system *Phys. Rev. Lett.* **103** 167003

[23] Sun Q and Xie X C 2009 Quantum transport through a graphene nanoribbonsuperconductor junctionm *J. Phys.: Condens. Matter* **21** 344204